NJC

PAPER

View Article Online
View Journal | View Issue

Cite this: *New J. Chem.*, 2015, 39, 482

Carbazole–corrole and carbazole–prophyrin dyads: synthesis, fluorescence and electrochemical studies†

Naresh Balsukuri, Sudipta Das and Iti Gupta*

Received (in Montpellier, France) 30th June 2014,
Accepted 27th October 2014

DOI: 10.1039/c4nj01086h

www.rsc.org/njc

Donor–acceptor type carbazole–corrole and carbazole–porphyrin dyads **4–9** were synthesized and characterized. Corrole and porphyrin containing one *meso*-*p*-iodophenyl group were coupled to *N*-butyl-3-ethynyl-carbazole by a modified Sonogashira reaction. All the dyads were characterized by HRMS mass, NMR, UV-vis absorption, fluorescence and electrochemical techniques. Fluorescence studies of dyads **4**, **7** and **8** indicated energy transfer from the donor carbazole moiety to the corresponding acceptor corrole/porphyrin moiety (up to 80%). The electron-releasing *N*-butyl-carbazole group affects the electronic properties of the corrole and porphyrin macrocycles in the dyads **4–9**. Electrochemical studies revealed that dyads **4** and **5** are difficult to reduce compared to their corresponding monomers, as reflected by the cathodic shift in their reduction potentials. Meanwhile, dyads **6–9** exhibited an anodic shift in their reduction potentials, suggesting that they are easy to reduce compared to their corresponding monomers.

1. Introduction

Corroles are porphyrin analogues, where four pyrrole rings are linked to each other *via* three methine bridges and one direct α–α linkage.[1] Corroles are aromatic macrocycles with a smaller cavity size, and the regular tautomer has three inner NH protons. Such qualities make corroles very good candidates for coordination with a variety of metal ions.[2] One pot synthesis of corroles has opened the door for the facile synthesis of much desired mono- and di-functionalized corroles.[3] These functionalized corroles can be further utilized to prepare covalently linked D–π–A (donor–acceptor) systems for various applications.[4] Jiang and coworkers[5] have reported phenothiazine–corrole dyads with enhanced quantum yields and tested their DNA photocleavage properties. Senge *et al.*[6] have reported the synthesis of carbazole bridged porphyrin dimers and their metal complexes, and utilized them further to make single layer organic light emitting diodes (OLEDs). Carbazole derivatives are well-known dyes with high electronic absorption and efficient fluorescent emission.[7,8] Due to their high photostability and elongated molecular shape, they have been used extensively in organic photovoltaics.[9,10] In recent years, *meso*-carbazole substituted porphyrins[11] and porphyrin dimers linked with carbazole[12] have been tested for dye-sensitized solar cell applications. A theoretical study by Ren and coworkers[13] on *meso*-carbazole substituted porphyrins revealed through-bond energy transfer in the system, where the carbazole group acts as a donor and the central porphyrin core acts as an acceptor. These authors also studied the highly efficient red light emitting properties of these compounds, which is associated with their covalently linked D–A type structures. Corroles are promising candidates for panchromatic dyes due to their intense absorption in the visible range, high fluorescent quantum yields and high radiative rate constants, meaning they can be linked with other chromophores to construct donor–acceptor type conjugated (D–π–A) systems.[4] Reports on light-harvesting arrays based on corroles are very few in number compared to analogous porphyrin arrays.[14,15] Thus, there is a need for corrole based multichromophoric arrays which are able to display energy/electron transfer properties. To the best of our knowledge, there is no report on carbazole units connected to corroles. In this report, we present the synthesis and characterization of dyads **4–6** and **7–9** which have one carbazole unit covalently attached to corrole and porphyrin, respectively. Steady state emission studies indicated the possibility of energy transfer from the donor-carbazole unit to the acceptor corrole/porphyrin unit in dyads **4**, **7** and **8**. Electrochemical studies of all the dyads revealed perturbation of the electronic properties of the corrole/porphyrin unit in these compounds. The corrole ring in dyads **4** and **5** is difficult to reduce compared to the free base corrole. On the contrary, the corrole or porphyrin ring is easy to reduce in dyads **6–9** compared to their corresponding monomers.

Indian Institute of Gandhinagar, VGEC Campus, Chandkheda, Ahmedabad-382424, India. E-mail: iti@iitgn.ac.in; Fax: +917923972324; Tel: +917932419502

† Electronic supplementary information (ESI) available. See DOI: 10.1039/c4nj01086h

2. Results & discussion

2.1 Synthesis of dyads 4–9

The starting materials corrole **1** and porphyrin **3** with one *p*-iodophenyl group were synthesized according to the procedures reported in the literature.[16,17] *N*-butylcarbazole with a mono-ethynyl functional group **2** was synthesized by following the reported method.[18] Synthetic routes for the carbazole–corrole and carbazole–porphyrin dyads are shown in Schemes 1 and 2, respectively. The carbazole–corrole dyad **4** was synthesized by the coupling of mono-iodophenylcorrole **1** with ethynylcarbazole derivative **2**, using $PdCl_2(PPh_3)_2$ as a catalyst in dry DCM/TEA, under a nitrogen atmosphere for 16 h.[19] The progress of the reaction was monitored by thin-layer chromatography (TLC), and a new green spot was observed below the corrole **1** on TLC in 50% DCM–petroleum ether. Column chromatographic purification of the crude mixture in 40% DCM–pet ether produced dyad **4** in 63% yield, as a greenish purple solid. The insertion of Cu into the corrole moiety of dyad **4** was achieved by reacting the dyad with copper acetate in pyridine.[20] Purification using a silica gel column in 15% DCM–pet ether afforded pure dyad **5** as a dark brown solid, in 89% yield. In dyad **5** the copper is present as Cu(III), and it is diamagnetic.[2] Similarly, dyad **6** was prepared by treating dyad **4** with cobalt acetate and triphenylphosphine in ethanol.[21] Pure dyad **6** was obtained after silica gel column purification in a 25% DCM–pet ether mixture, in 56% yield. Porphyrin–carbazole dyad **7** was prepared by following Lindsey's modified palladium coupling procedure.[22] Mono-iodophenylporphyrin **3** was coupled with ethynylcarbazole derivative **2** in toluene/TEA at RT in the presence of $Pd_2(dba)_3/AsPh_3$ for 16 h under an inert atmosphere. Purification of the crude dyad by a neutral alumina column using a 30% DCM–pet ether mixture afforded dyad **7**, in 61% yield. The porphyrin–carbazole dyad **7** was subjected to Zn metallation by a reaction with zinc acetate, in $CHCl_3$–MeOH as the solvent mixture.[23] Pure dyad **8** was obtained as a pink solid in 76% yield, by neutral alumina column chromatography in a 40% DCM–pet ether mixture. Dyad **9** was synthesized by refluxing dyad **7** with copper acetate in a DCM/MeOH (1 : 1) mixture for 1 h.[24] Purification of the crude dyad on a neutral alumina column with a 25% DCM–pet ether mixture produced dyad **9** as a red solid, in 62% yield.

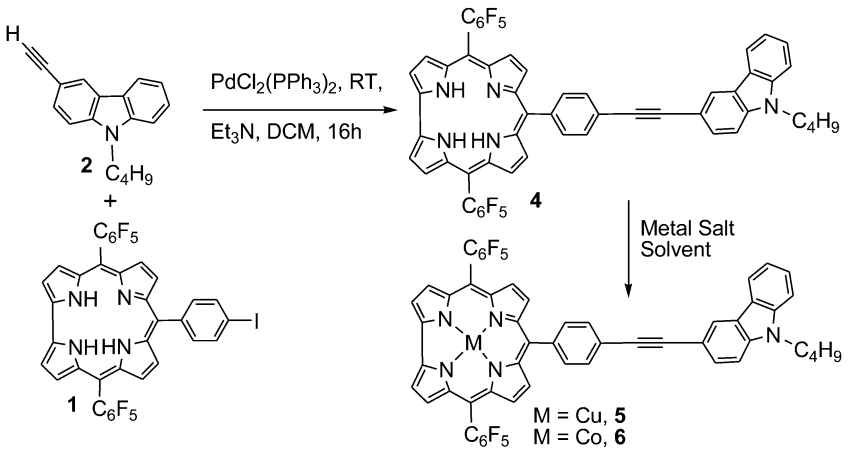

Scheme 1 Synthesis of carbazole–corrole dyads.

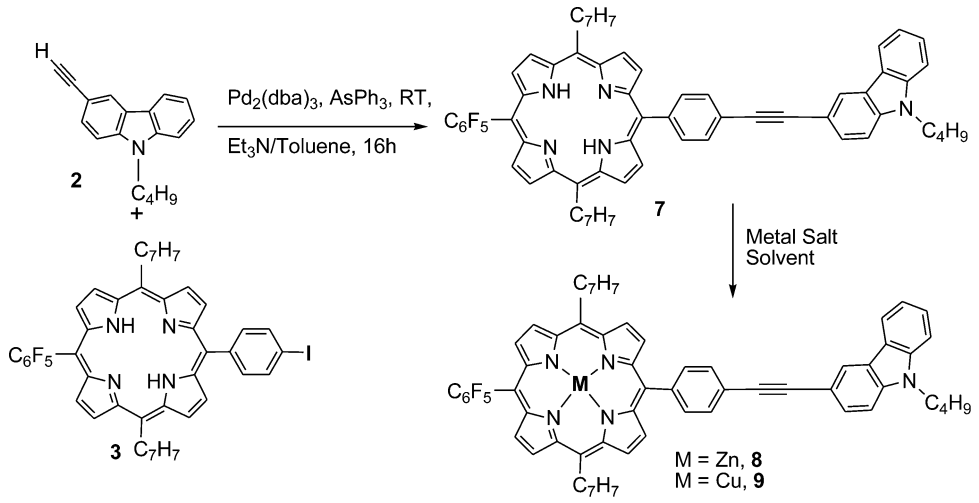

Scheme 2 Synthesis of carbazole–porphyrin dyads.

All the dyads were characterized with ^{1}H-NMR, UV-vis and ESI-Q-TOF or MALDI-mass fluorescence and electrochemical techniques. The M^+ ion peak at m/z 952.2498 in the ESI mass spectra (ESI-MS) confirmed the formation of corrole–carbazole dyad **4**. The dyads **5** and **6** were confirmed by molecular ion peaks at m/z 1011.135 and 1006.802 in the ESI-MS and the MALDI mass spectra (MALDI-MS), respectively. Similarly, three other dyads **8–9** were also confirmed by molecular ion peaks in mass spectrometry (ESI).

The resonances in the ^{1}H NMR spectra of dyads **4–8** were assigned by comparing them with the ^{1}H NMR data of their corresponding monomers. Dyad **9** has Cu(II) metal in the porphyrin centre, making it paramagnetic in nature, and thus ^{1}H-NMR was not recorded for this dyad. The NMR spectral features of dyads **4–8** were a combination of their corresponding constituting monomers. In the ^{1}H NMR of dyad **4** the eight β-pyrrole protons showed up as three sets of signals at 9.11, 8.74 and 8.57 ppm, while the four aryl protons of the corrole moiety showed up as two distinct doublets at 8.18 and 7.98 ppm. The seven carbazole aromatic protons appeared as four sets of signals at 8.41, 8.11, 7.75 and 7.43 ppm, and the nine protons of the *N*-butyl group showed up as four sets of signals at 4.31, 1.89, 1.42 and 0.98 ppm. In the ^{1}H NMR of dyad **6** the eight β-pyrrole protons showed up as four sets of signals at 8.72, 8.32, 8.25 and 8.03 ppm, and the four aryl protons of the corrole moiety showed up as four set of signals at 8.06, 7.85, 7.79, and 7.28 ppm. The seven carbazole aromatic protons appeared as seven sets of signals between 8.41 to 7.27 ppm, while the nine protons of the *N*-butyl group showed up as four sets of signals at 4.33, 1.88, 1.44 and 0.97 ppm. The fifteen axial phenyl protons showed up as three sets of signals at 7.03, 6.68 and 4.64 ppm. Additionally, the ^{1}H–^{1}H COSY spectrum of dyad **6** was recorded in $CDCl_3$ and is presented in the ESI.† The NMR signals of dyad **5** were slightly broader due to the Cu(III) metal center, which reaches an equilibrium with the Cu(II) complex of the corrole π-cation radical.[2] In the ^{1}H NMR of dyad **7** the eight β-pyrrole protons of the porphyrin moiety showed up as three sets of signals at 8.96, 8.89, and 8.76 ppm, and the twelve aryl protons of the porphyrin moiety showed up as four sets of doublets at 8.20, 8.09, 7.96 and 7.56 ppm. The seven carbazole aromatic protons appeared as six sets of signals between 8.44 to 7.27 ppm, while the NMR signal pattern of the nine protons of the *N*-butyl group was similar to that of dyad **4** described earlier. The ^{1}H NMR pattern of dyad **8** with Zn(II) metal in the porphyrin ring was very similar to that of dyad **7**, although the β-pyrrole peaks were slightly downfield shifted compared to dyad **7**. The NMR analysis of all the dyads with comparisons to their corresponding monomers, suggests weak interactions between the corrole or porphyrin and the carbazole moieties.

2.2 Absorption properties

Carbazole is an electron-rich moiety which absorbs in the range of 290–450 nm and may act as electron/energy donor in the dyad. Meanwhile, corrole and porphyrin absorb in the range of 400–700 nm and may act as electron/energy acceptors in the dyads. UV-vis spectra of dyads **4–9** and their corresponding monomer units, corrole **1** and porphyrin **3** were recorded in toluene; the data are presented in Table 1. Absorption spectra of the corrole based dyads **4–6** and their corresponding monomers are shown in Fig. 1. The absorption spectra of the dyads are a linear combination of the spectra of their corresponding monomers. For example, dyad **4** showed one Soret band at 424 nm and three ill-defined Q-bands at 565, 616 and 645 nm, which are overlapping with the monomer **1**.[25] The absorption band at 297 nm in dyad **4** corresponds to the *N*-butylcarbazole moiety.[26]

The absorption spectra of the porphyrin based dyads **7–9** and their corresponding monomers are shown in Fig. 2. Dyad **6** showed a split Soret band at 383 and 413 nm along with two Q bands at 560 and 589 nm, compared to the single Soret and Q bands of Co-TPC[19] (Table 1). Similarly, dyad **7** showed major absorption bands at 300 and 422 nm, corresponding to *N*-butylcarbazole and porphyrin **3** respectively. The wavelengths of absorption of the four Q-bands in dyad **7** also matched those of the monomer porphyrin **3**.[27] A close look at Table 1 and Fig. 2 clearly shows only minor changes in the band shapes and wavelength maxima for all the dyads **4–9** compared to their corresponding monomers. This observation reflects that the two monomeric units retain their individual identities, and interact weakly in the dyads.

2.3 Fluorescence properties

Steady state fluorescence spectral studies for dyads **4**, **7** and **8** were carried out in toluene. The fluorescence quantum yields (Φ_f) of dyads **4** and **7** were estimated from the emission and absorption spectra by a comparative method, using H_2TPP ($\Phi_f = 0.11$) as a standard, in toluene.[28] For fluorescence quantum yield calculation of dyad **8**, ZnTPP (Φ_f = 0.033) was used as a

Table 1 UV-vis absorption data of the dyads, recorded in toluene. The concentration was 10^{-5} M

Compound	Other	Soret band λ (nm) ($\log\varepsilon$)		Absorption Q-bands λ (nm) ($\log\varepsilon$)		
CuTPP		414 (5.66)		538 (4.28)	574 (—)	—
CuTPC		410 (5.09)		538 (3.89)	—	—
Co-TPC		386 (—)		562 (—)	—	—
Corrole **1**	—	421 (5.86)	—	583 (4.97)	613 (4.87)	644 (4.71)
Porphyrin **3**	—	420 (5.81)	514 (4.47)	548 (3.89)	591 (3.69)	646 (2.74)
Dyad **4**	297 (5.48)	424 (5.84)	—	565 (5.02)	616 (4.79)	645 (4.65)
Dyad **5**	296 (5.68)	410 (5.87)	—	558 (5.02)	—	630 (4.74)
Dyad **6**	297 (5.89), 383 (5.94)	413 (5.96)	—	560 (5.26)	589 (5.19)	—
Dyad **7**	300 (4.94)	422 (5.84)	515 (4.52)	551 (5.11)	591 (3.79)	647 (3.39)
Dyad **8**	301 (4.95)	426 (5.91)	—	—	551 (4.63)	590 (3.72)
Dyad **9**	301 (5.02)	420 (5.85)	—	—	541 (4.52)	571 (3.12)

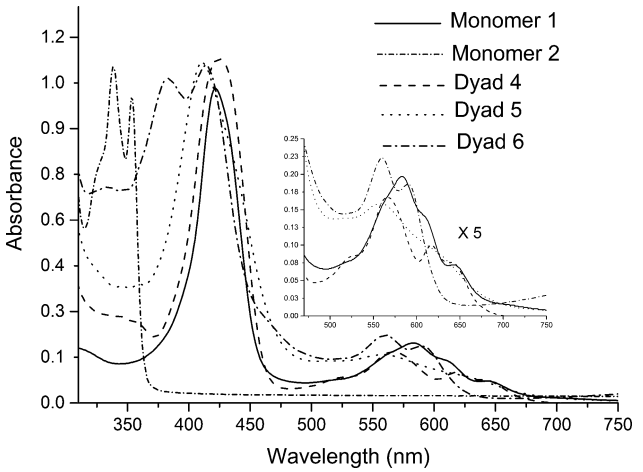

Fig. 1 Comparison of the absorption spectra of dyads **4–6** and their corresponding monomers, recorded in toluene. The inset shows the expanded Q-bands.

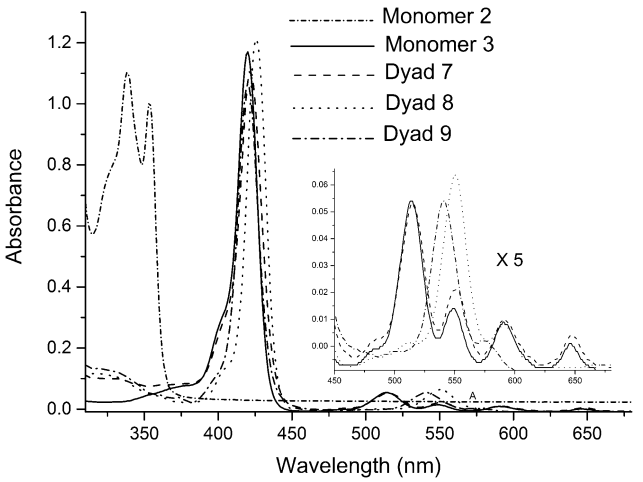

Fig. 2 Comparison of the absorption spectra of dyads **7–9** and their corresponding monomers, recorded in toluene. The inset shows the expanded Q-bands.

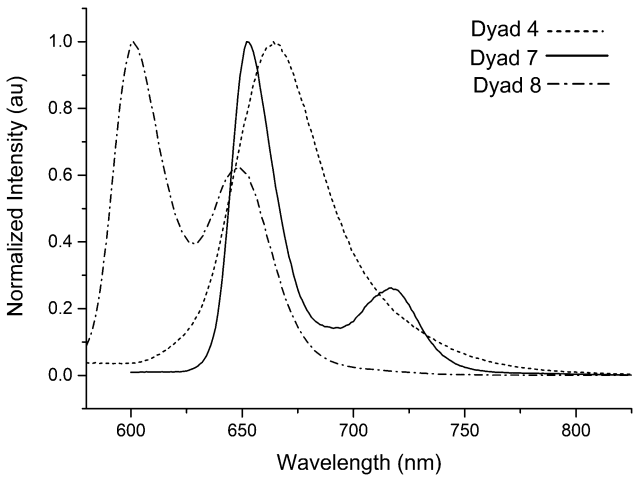

Fig. 3 Comparison of normalized emission spectra of dyads **4** (λ_{ex} = 424 nm), **7** (λ_{ex} = 515 nm) & **8** (λ_{ex} = 550 nm) in toluene.

Table 2 Fluorescence data for the dyads recorded in toluene

Compound	Excitation (λ_{ex})/nm	Emission (λ_{em})/nm	Donor (Φ_f)	Acceptor (Φ_f)	ETE (%)
H_2TPP[a]	515	654, 717	—	0.11	—
H_3TPC[b]	414	667	—	0.19	—
Monomer **2**[c]	330	372, 385	0.127	—	—
ZnTPP[d]	550	597, 647	—	0.033	—
Dyad **4**	424	662	—	0.19	—
	300	366, 438, 662	0.048	0.14	74
Dyad **7**	515	654, 718	—	0.099	—
	300	398, 453, 652, 717	0.055	0.05	51
Dyad **8**	550	601, 649	—	0.049	—
	270	600, 645	ND	0.039	80

[a] Taken from ref. 28. [b] Taken from ref. 25. [c] λ_{ex} = 330 nm in toluene; anthracene (Φ_f = 0.25 in ethanol) was used as a standard. [d] Taken from ref. 29.

standard.[29] Fluorescence quantum yield measurement for dyads **5**, **6** and **9** was not possible due to their very weak emissions or non-fluorescent natures. A comparison of the emission spectra of dyads **4**, **7** and **8** is shown in Fig. 3 and the data are presented in Table 2. The emission maximum of dyad **4** was comparable with the H_3TPC and the quantum yield of the corrole unit in dyad **4** was comparable to that of H_3TPC.[25] The quantum yields and emission maxima of the porphyrin and Zn–porphyrin units in dyads **7** and **8**, respectively, were comparable to their corresponding monomers (Table 2). The fluorescence studies of dyads **4**, **7** and **8** indicated weak interactions between the carbazole and the porphyrin/corrole units in these compounds.

Since the carbazole moiety absorbs between 300–400 nm and corrole/porphyrin absorbs around 420–650 nm, an energy transfer from the carbazole moiety to the corrole/porphyrin core is expected. Fluorene (donor) linked to porphyrin (acceptor) by conjugated chemical linkages has been shown to exhibit through-bond energy transfer.[30] Also, such systems have been reported to be efficient non-doped red light emitting materials, useful for red OLEDs.[31] Similar to fluorene linked porphyrin systems, all three dyads **4**, **7** and **8** exhibited energy transfer phenomena from the donor carbazole unit to the acceptor corrole/porphyrin core. A comparison of the emission spectra of dyad **4**, *N*-butylcarbazole and a 1 : 1 mixture of *N*-butyl carbazole and corrole **1** is shown in Fig. 4. The *N*-butylcarbazole and corrole **1** molecules emit in the ranges of 340–450 nm and 640–750 nm, respectively. As shown clearly in Fig. 4, upon excitation of a 1 : 1 mixture of monomer **2** and corrole **1** at 300 nm, where *N*-butylcarbazole absorbs strongly, emission was observed exclusively from *N*-butylcarbazole between 380–480 nm, and no emission was observed from corrole **1**. However, in the case of dyad **4**, the excitation of the *N*-butylcarbazole unit at 300 nm resulted in a weak, and slightly red-shifted, emission from the carbazole unit between 390–500 nm (Fig. 4). The sharp peak observed at exactly 600 nm in the emission spectrum of dyad **4** was due to scattering from the fluorescence instrument, and it had been avoided during quantum yield calculations of the acceptor unit in the dyad. Strong emission at 662 nm was also observed, which corresponds to the corrole unit in dyad **4**. This donor-to-acceptor energy transfer could

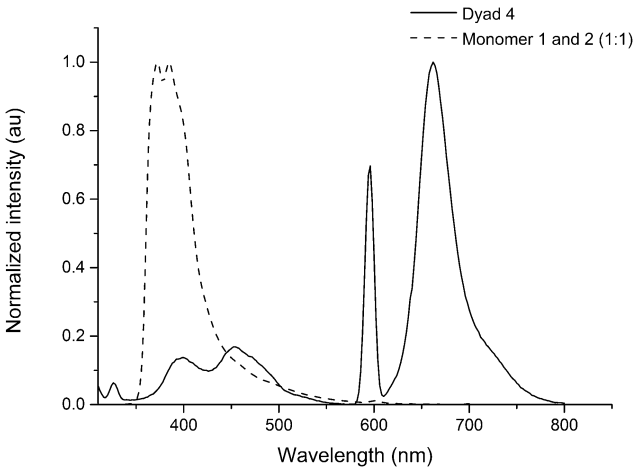

Fig. 4 Comparison of the normalized emission spectra of dyad **4** and a 1 : 1 mixture of monomer **2** and corrole **1** in toluene (λ_{ex} = 300 nm). The sharp peak at 600 nm is due to scattering, which is observed at exactly double the excitation wavelength of 300 nm (second order diffraction through emission monochromator in the fluorescence instrument).

be due to through-bond transfer, or another mechanism. The "energy transfer efficiency" (ETE, %) is a measure of total energy transfer irrespective of the mechanism, and it can be calculated as follows:

$$\mathrm{ETE}\% = \frac{\phi_f \text{ of acceptor in the molecule excited at the donor}}{\phi_f \text{ of acceptor in the molecule excited at the acceptor}} \times 100$$

The quantum yields of the corrole/porphyrin (acceptor) units in the dyads **4**, **7** and **8** were calculated at two different wavelengths *i.e.* excited at donor (*meso*-carbazole, 300 nm), and excited at acceptor (corrole/porphyrin core, 424, 515 and 550 nm respectively). The data are given in Table 2. The ETE gives an idea of the extent of the energy transfer, including the loss in energy by non-radiative process in the energy transfer.[32] The calculated values of ETE (%) are: dyad **4** (74%), dyad **7** (51%) and dyad **8** (80%). The energy transfer through bond[33,34] might be possible, as the emission maxima of the donor and acceptors were not altered significantly (ESI). Additionally, the quantum yields of the acceptor units (corrole/porphyrin) in dyads **4**, **7** and **8** were not much affected when excited at the acceptors' wavelengths. However, the quantum yields of the donor carbazole moiety were reduced by half in dyads **4** and **7** compared to the reported value of *N*-alkylcarbazole.[35] In the case of dyad **8**, carbazole emission (ESI) was not detected upon excitation at the donor wavelength (270 nm), and only zinc–porphyrin unit emission was observed. The reduced quantum yields of the carbazole moiety upon excitation at the donor wavelength in dyads **4**, **7** and **8** suggest an efficient energy transfer from the carbazole unit to the corrole/porphyrin unit (Table 2) in these compounds.

2.4 Time resolved fluorescence measurements

The singlet excited state lifetimes τ of dyads **4**, **7** and **8** and the associated reference compounds, monomer **2**, H_2TPP H_3TPC and ZnTPP, were monitored using a time-resolved fluorescence technique. The dyads **4**, **7** and **8** were excited both at 406 nm and at 330 nm, corresponding to their monomeric porphyrin/corrole and *N*-butylcarbazole moieties. The data were collected at different wavelengths corresponding to the emission peak maxima of the donor (*N*-butylcarbazole) and the acceptor (porphyrin/corrole) in the dyads. The fluorescence decay profiles and weighted residuals of dyads **4**, **7** and **8** are presented in Fig. 5 and the data are tabulated in Table 3. The fluorescence decays of the corrole/porphyrin units in the dyads were fitted to a single exponential and the observed lifetimes were 4.0 ns (for the corrole unit in dyad **4**), 9.3 ns (for the porphyrin unit in dyad **7**) and 2.0 ns (for the Zn–porphyrin unit in dyad **8**). The fluorescence decays of dyads **4**, **7** and **8** collected at the *N*-butylcarbazole unit (384 nm) were fitted to a double exponential, and the observed lifetimes τ_1 (corresponding to the *N*-butylcarbazole unit) were reduced in the dyads as compared to the free monomer **2**, which had a lifetime of 8.89 ns (Table 3). The other minor components of the fluorescence decays of dyads **4**, **7** and **8** were attributed to the monomeric porphyrin impurities present in the dyads. The major short components for dyads **4**, **7** and **8** observed at 1.23 ns, 1.36 ns and 1.14 ns, respectively, were attributed to the *N*-butylcarbazole unit in the dyads. The quenched lifetimes of *N*-butylcarbazole in dyads **4**, **7** and **8** respectively, compared to that of free monomer **2** (Table 3), were due to the singlet–singlet excitation energy transfer from the *N*-butylcarbazole unit to the porphyrin/corrole unit. The rate of energy transfer (k_{ENT}) and the efficiency of energy transfer (ϕ_{ENT}) were calculated[34] in dyads **4**, **7** and **8** using the following equations:

$$k_{ENT} = 1/\tau_{DA} - 1/\tau_D \quad (1)$$

$$\phi_{ENT} = k_{ENT} \times \tau_{DA} \quad (2)$$

The k_{ENT} and ϕ_{ENT} values calculated for dyads **4**, **7** and **8** were (1429 ps^{-1}, 86%), (1606 ps^{-1}, 85%) and (1308 ps^{-1}, 87%)

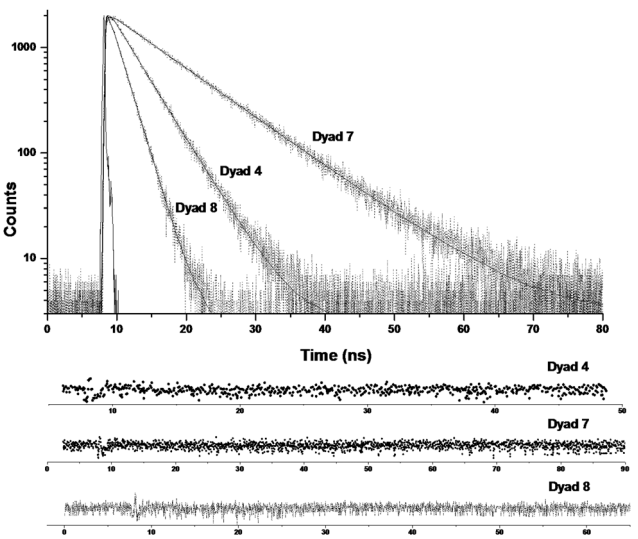

Fig. 5 Fluorescence decays and weighted residuals of dyads **4**, **7** and **8** (λ_{ex} = 405 nm).

Table 3 Singlet excited state lifetimes of dyads **4**, **7**, **8** and monomers in toluene

Compound	λ_{ex} [a]	$\lambda_{em\ (max)}$ [b]	τ_1 (ps)	τ_2 (ps)
Monomer 2	330	384	8890	—
H_3TPC	405	667	3890	—
H_2TPP	405	654	9200	—
ZnTPP	405	597	2044	—
Dyad **4**	405	664	4006	—
Dyad **7**	405	652	9351	—
Dyad **8**	405	601	2044	—
Dyad **4**	330	384	1230[c]	6700[d]
Dyad **7**	330	384	1360[c]	5900[d]
Dyad **8**	330	384	1140[c]	6050[d]

[a] Laser excitation source wavelength. [b] Data collected at their respective emission maxima. [c] These data fitted to biexponential curve. [d] These data fitted to biexponential curve.

Table 4 Through-bond (TB) and through-space (TS) energy transfer rates and contributions for dyads

Compound	J[a] ($cm^6\ mmol^{-1}$)	k_{ENT}^{-1} (ps)	ϕ_{ENT}	k_{TS}^{-1} (ps)	k_{TB}^{-1} (ps)	χ_{TB}	χ_{TS}
Dyad **4**	1.24×10^{-13}	1428	0.86	32 456	1492	0.95	0.05
Dyad **7**	9.17×10^{-14}	1606	0.85	24 002	1754	0.91	0.09
Dyad **8**	8.07×10^{-14}	1308	0.87	21 123	1402	0.93	0.07

[a] Spectral overlap term calculated by using PhotochemCAD software (ref. 31, see ESI).

respectively (Table 4). The TS energy transfer contribution can be evaluated in terms of the Förster mechanism.[34] The Förster process is mediated by the donor–acceptor distance and orientation as well as their emission and absorption spectral overlap characteristics (J, spectral overlap term, Table 4). According to Förster's theory, the energy transfer rates can be calculated by the following equation:

$$k_{TS} = (8.8 \times 10^{23})K^2\phi_D J\, n^{-4}\tau_D^{-1}R^{-6} \quad (3)$$

where K is the orientation factor (1.125), ϕ_D is the fluorescence quantum yield of the donor in the absence of the acceptor, J is the spectral overlap integral (calculated by PhotochemCAD,[36–38] see ESI†), n is the solvent refractive index (1.49 for toluene), τ_D is the donor lifetime in the absence of the acceptor and R is the center-to-center donor–acceptor distance in the dyads.

The optimized value of R was calculated by DFT theory using a B3LYP functional and a 6-31G(d) basis set. The minima of molecular structure were confirmed by Hessian calculation. The center-to-center donor–acceptor distance was found to be 15.16 Å in dyad **4**. The same distance (15.2 Å) was used for the energy transfer calculations in the other two dyads **7** and **8**. Through-space energy transfer rates (k_{TS}), and the relative contributions of TS (χ_{TS}) and TB (χ_{TB}) energy transfer to the overall rate were calculated using the following equations:

$$k_{ENT} = k_{TB} + k_{TS} \quad (4)$$

$$\chi_{TS} = k_{TS}/k_{ENT} \quad (5)$$

$$\chi_{TB} = k_{TB}/k_{ENT} \quad (6)$$

The data are summarized in Table 4. An inspection of Table 4 reveals from the energy transfer rates and efficiencies that dyads **4**, **7** and **8** were much slower and less efficient than the porphyrin dyads reported by Lindsey's group[39–41] and Osuka *et al.*[42] The rates of TB energy transfer in dyads **4**, **7** and **8** were in a range of 1.4 to 1.8 ns^{-1} and the rates of TS energy transfer were in a range of 21–32 ns^{-1}. The TS rates were much slower and the TB contribution accounts for greater than 90% of the observed rate. The observed rates of energy transfer are quite slow in **4**, **7** and **8**, which could be partially attributed to the presence of two or one pentafluorophenyl groups at the *meso*-position of the acceptor corrole/porphyrin unit in the dyads. This is in agreement with the observation that the *meso*-pentafluorophenyl groups affect the electronic communication in *meso–meso* linked porphyrin dyads, resulting in slow energy transfer rates.[40] The porphyrin dyad with six *meso*-pentafluorophenyl groups had ten times slower rates of energy transfer than that of porphyrin dyads with six *meso*-mesityl groups at their periphery.[41] The slower energy transfer rates could also be due to the bent position of the carbazole donor in the reported dyads. As was observed earlier, that the attachment of the donor group to the acceptor porphyrin *via* a *meta*/*para* linker can alter the electronic communication, resulting in the reduced energy transfer rates in *meta*-linked porphyrin dyads.[41] Another important factor is that the coplanarity of the linker, with respect to the donor and acceptor units, in porphyrin dyads increases the electronic communication, thereby affecting the rates of energy transfer.[41] Additionally, the TS contributions estimated for dyads **4**, **7** and **8** (Table 4) were also found to be very minor, supporting the predominant contribution of TB only. Thus, the carbazole donor units linked *via* a phenylethyne bridge to a porphyrin or corrole unit in the reported dyads have three factors: (i) a short linker compared to diphenylethyne bridged systems; (ii) a non-coplanar (bent) linker between D and A; (iii) electron-withdrawing C_6F_5 groups at the *meso* position of the corrole/porphyrin unit. All these factors affected the electronic communication between D and A, and resulted in slower energy transfer rates in the dyads.

2.5 Electrochemical properties

The cyclic voltammetric measurements of dyads **4–9** were carried out under a nitrogen atmosphere at a scan rate of 50 mV s^{-1} using 0.1 M tetrabutylammonium perchlorate as the supporting electrolyte. The redox potential data for all the dyads and a comparison of the oxidation and reduction waves are shown in Table 5 and Fig. 6, respectively. The presence of an electron-rich carbazole moiety in the dyads is expected to shift the redox potentials of corrole or porphyrin unit. Therefore, it is important to characterize the electrochemical behavior of these dyads. The reported CV of Corrole **1**[19] comprised of four oxidation processes and one irreversible reduction (Table 5). The dyad **4** showed two irreversible oxidations at 1.05 and 1.31 V along with two reduction processes, one reversible at −0.73 V and one irreversible at −1.61 V. Whereas, the free base corrole **1** showed three oxidations and only one reduction wave (Table 5). Copper containing dyad **5** displayed three irreversible

Table 5 Electrochemical redox data (V) of dyads **4–9** in dichloromethane, containing 0.1 M TBAP as the supporting electrolyte, recorded at a 50 mV s^{-1} scan speed

	$E_{1/2}$(oxd)/V *vs.* SCE			$E_{1/2}$(red)/V *vs.* SCE			
Compound	I	II	III	I	II	III	Ref.
Corrole **1**	0.03, 0.50	0.86	1.39	−0.24	—	—	19
Dyad **4**	1.05	1.31	—	−0.73	−1.61	—	This work
CuTPC	0.76	—	—	−0.20	—	—	20
Dyad **5**	0.16	1.07	1.62	−0.74	−1.10	−1.70	This work
CoTPC	0.51	0.92	1.56	−0.75	−1.61	—	43
Dyad **6**	0.79	1.23	—	−0.44	−1.37	—	This work
H_2TTP	—	1.03	1.30	—	−1.23	−1.55	44
Dyad **7**	—	1.24	1.69	−0.99	−1.36	−1.58	This work
ZnTTP	0.80	1.09	—	—	−1.25	−1.67	44
Dyad **8**	0.97	1.25	—	—	−1.15	−1.56	This work
CuTPP	0.97	1.35	—	—	−1.30	−1.70	44
Dyad **9**	—	1.21	1.36	—	−1.13	−1.61	This work

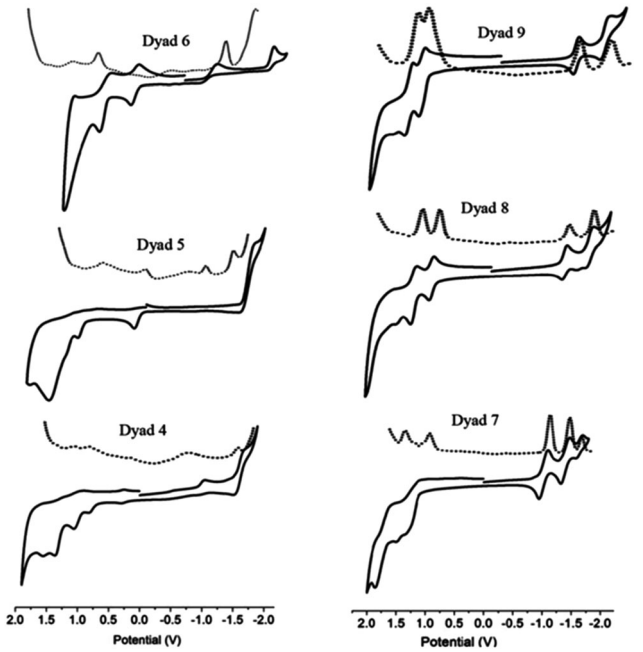

Fig. 6 Comparison of the cyclic voltammograms (solid lines) and differential pulse voltammograms (dashed lines) of dyads **4–9**, in DCM containing 0.1 M TBAP as a supporting electrolyte, recorded at a 50 mV s^{-1} scan speed (V *vs.* SCE).

oxidations ranging from 0.16 to 1.62 V and three irreversible reductions between −0.74 to −1.7 V. On the other hand, copper corrole (Cu-TPC)[20] had shown only one oxidation and one reduction wave (Table 5). Cobalt corrole was reported to have three oxidations processes between 0.51 to 1.56 V and two reductions around −0.75 and −1.61 V.[43] The cobalt containing dyad **6** exhibited two oxidations processes, one quasi-reversible at 0.79 V and one reversible at 1.23 V. Dyad **7** having free base porphyrin unit, undergoes two irreversible oxidations at 1.24 and 1.69 V along with three reductions processes in between −0.99 to −1.58 V. While H_2TPP displayed two oxidations peaks at 1.03 and 1.30 V in addition to the two reductions processes at −1.23 and −1.55 V.[44] Dyad **8** with zinc metal exhibited two reversible oxidations at 0.97 and 1.25 V along with one reversible reduction at −1.15 V and one quasi-reversible one at −1.56 V. Dyad **9** with copper metal displayed two oxidations, one quasi-reversible and one reversible at 1.21 V and 1.36 V respectively. Also dyad **9** showed one reversible reduction at −1.13 V and one quasi-reversible reduction at −1.61 V. The oxidation and reduction potential values of dyads **4–9** are very different from their corresponding monomers, suggesting that the coupling with the carbazole moiety at the *meso* position affected the electronic properties of the corrole/porphyrin units in all the compounds. In the case of dyad **4** the reduction potentials are shifted to a more negative state, indicating that it is difficult to reduce the corrole ring in dyad **4** compared to the free base corrole **1**. Similarly, for dyad **5** the reduction potential values are more negative than that of copper corrole (CuTPC), suggesting that dyad **5** is difficult to reduce compared to CuTPC. On the contrary, dyad **6** is easy to reduce and difficult to oxidize compared to cobalt corrole (CoTPC), as reflected by the anodic shift of the reduction potentials (Table 5). In the case of dyads **7**, **8** and **9** the oxidation potentials experienced anodic shifts, suggesting that it is difficult to oxidize the porphyrin ring in the dyads compared to their corresponding monomers.

3. Conclusions

In conclusion, carbazole–corrole and carbazole–porphyrin dyads and their metal complexes were synthesized and studied using electrochemical and fluorescence techniques. Fluorescence studies indicated the efficient energy transfer from the donor-carbazole moiety to the acceptor units, corrole or porphyrin, in dyads **4**, **7** and **8**. The presence of a bent phenylethyne linker between the D and A units in the dyads, and pentafluorophenyl groups at the *meso*-position of the corrole/porphyrin unit in the dyads, resulted in slower rates of energy transfer with reduced efficiencies of energy transfer. Varying the position of the linker and attachment of the donor carbazole moiety to the acceptor unit within the dyads may produce highly efficient energy transfer systems for different applications. In addition, the linkage of an electron-rich carbazole moiety to the corrole or porphyrin unit affected their electronic properties in the dyads, as judged by cyclic voltammetry. Dyads **4** and **5** showed cathodic shifts whereas dyads **6–9** exhibited anodic shifts in their reduction potentials, compared to their corresponding monomers.

4. Experimental

4.1 Instrumentation and reagents

Unless otherwise mentioned, all the reagents and solvents were purchased from Aldrich, Acros Organics or Merck and were used without further purification. Pyrrole was distilled under vacuum prior to use. Silica gel (60–120 mesh size) and neutral alumina (Brockmann Grade I-II) used for column chromatography were procured from Merck. The solution NMR spectra of

compounds were recorded with a BrukerAvance III 500 MHz NMR spectrometer at IIT Gandhinagar. The HRMS data for all the compounds (except for **5**, **8** and **9**) were recorded (in positive ion mode) with a Waters Synapt-G2S ESI-Q-TOF Mass instrument at IIT Gandhinagar. MALDI MS data for compound **5**, **8** and **9** were recorded on a BrukerDaltonics MALDI-TOF instrument at Kyushu University. Absorption spectra were recorded with Shimadzu UV-1700 and fluorescence emission studies were performed using a Horiba-JobinYvon Fluolorog-3 Spectrometer at IIT Gandhinagar. The time-resolved fluorescence decay measurements were carried out at IIT Gandhinagar using a pico-second-diode-laser-based, time-correlated, single-photon counting (TCSPC) fluorescence spectrometer from Edinburgh Instruments Ltd., LifespecII, (Livingston, UK). Cyclic voltammetry (CV) and differential pulse voltammetry (DPV) studies were carried out with an electrochemical system utilizing the three electrode configuration consisting of glassy carbon (working electrode), platinum wire (auxiliary electrode) and saturated calomel (reference electrode) electrodes. The experiments were done under a nitrogen atmosphere in dry DCM using 0.1 M tetrabutylammonium perchlorate as the supporting electrolyte at IIT Bombay. Half wave potentials were measured using DPV and also calculated manually by taking the average of the cathodic and anodic peak potentials. All potentials were calibrated *vs.* saturated calomel electrode by the addition of ferrocene as an internal standard, taking $E_{1/2}$ (Fc/Fc^+) = 0.51 V *vs.* SCE.

4.2 Synthesis

Mono-iodophenylcorrole **1**[13] and 3-ethynyl-9-butylcarbazole **2**[15] were prepared according to the reported procedures.

Mono-iodophenylporphyrin 3. 1,9-Bis-(4-methylbenzoyl)-5-(pentafluorophenyl)dipyrromethane (200 mg, 0.364 mmol) was added to a dry round-bottomed flask (RB) and THF/MeOH (2 : 3, 50 mL) was added to the RB. $NaBH_4$ (2 g, 54.7 mmol) was added to it in several portions at 0 °C for 30 min, and after that the reaction mixture was stirred for 45 min at room temperature. The reaction was stopped when a new spot corresponding to diol was observed on the TLC ($KMnO_4$ dye was used to visualize the spot). Then the reaction mixture was extracted with ethylacetate and dried over Na_2SO_4 for 1 h. After this, the solvent was evaporated under reduced pressure on a rotary evaporator. The resultant dipyrromethanediol (200 mg, 0.36 mmol) was mixed with 5-(4-iodophenyl)dipyrromethane (126.03 mg, 0.361 mmol) in 145 mL of CH_3CN. TFA (0.327 mL, 4.392 mmol) was added into the reaction mixture and it was stirred for 2 h at room temperature. Then DDQ (245.85 mg, 1.083 mmol) was added to the reaction mixture and it was left under stirring for another hour. The reaction was quenched by adding TEA (0.6 mL). The crude porphyrin was subjected to neutral alumina column chromatography and desired porphyrin **3** was eluted with a 25% DCM–petroleum ether mixture. The solvent was evaporated to afford porphyrin **3** as a red-pink solid, in 11% yield (32 mg). Mp > 300 °C; R_f = 0.28 (silica, DCM–hexane 1 : 5); ^{1}H NMR ($CDCl_3$, 500 MHz, δ ppm): 8.99 (d, J = 4 Hz, 2H, β-pyrrole), 8.91 (d, J = 3.8 Hz, 2H, β-pyrrole), 8.85 (d, J = 3.8 Hz, 2H, β-pyrrole), 8.79 (d, J = 3.7 Hz, 2H, β-pyrrole), 8.12 (d, J = 7 Hz, 6H, Ar), 7.96 (d, J = 7.8 Hz, 2H, Ar), 7.6 (d, J = 7.4 Hz, 4H, Ar), 2.74 (s, 6H, Ar–CH_3), −2.75 (s, 2H, inner NH); ^{13}C NMR ($CDCl_3$, 500 MHz, δ ppm): 141.59, 137.72, 136.11, 135.88, 134.53, 127.58, 121.18, 120.28, 100.28, 94.32, 29.72, 21.54; HRMS (ESI-Q-TOF): $C_{46}H_{29}N_4IF_5^+$ $[M + H]^+$ calcd m/z 858.1279, found. m/z 859.1409.

Dyad 4. To a clean and dry 3-necked 50 mL round-bottomed flask 5-(4-iodophenyl)-10,15-bis-(pentafluorophenyl)corrole **1** (50 mg, 0.06 mmol) and 3-ethynyl-9-butylcarbazole **2** (29.71 mg, 0.12 mmol) were added under a nitrogen atmosphere. Dry DCM (18 mL) and dry TEA (9 mL) were added to the RB. After 10 min. $Pd(PPh_3)_2Cl_2$ (5.49 mg, 0.006 mmol) was added and the reaction mixture was stirred at RT for 16 h. The reaction was stopped when, after checking the TLC, a new green spot was detected. The solvent mixture was evaporated under reduced pressure on a rotary evaporator. The crude product was purified by column chromatography on neutral alumina, and the desired dyad was collected in a 40% DCM–pet ether mixture; evaporation of the solvents afforded dyad **4** as a greenish purple solid, in 63% yield (36 mg). Mp > 300 °C; R_f = 0.26 (silica, DCM–hexane 1 : 3); ^{1}H NMR ($CDCl_3$, 500 MHz, δ ppm): 9.11 (d, J = 3.5 Hz, 2H, β-pyrrole), 8.74 (d, J = 4 Hz, 4H, β-pyrrole), 8.57 (s, 2H, β-pyrrole), 8.41 (s, 1H, carbazole Ar), 8.18 (d, J = 7.5 Hz, 2H, Ar), 8.11 (d, J = 7.5 Hz, 1H, carbazole Ar), 7.98 (d, J = 7.5 Hz, 2H, Ar), 7.75 (d, J = 8.5 Hz, 1H, carbazole Ar), 7.43 (m, 4H, carbazole Ar), 4.31 (t, J = 7 Hz, 2H, N–CH_2), 1.89 (m, 2H, CH_2), 1.42 (m, 2H, CH_2), 0.98 (m, 3H, CH_3); ^{13}C NMR ($CDCl_3$, 500 MHz, δ ppm): 140.82, 140.23, 134.74, 136.89, 134.74, 130.44, 129.33, 126.11, 124.18, 122.92, 122.44, 120.51, 119.36, 118.60, 113.12, 112.88, 108.94, 108.83, 102.04, 87.49, 43, 31.12, 26.63, 20.58, 13.89; HRMS (ESI-Q-TOF): $C_{55}H_{32}N_5F_{10}^+$ $[M + H]^+$: calcd m/z 952.2498, found. m/z 952.2339.

Dyad 5. Dyad **4** (20 mg, 0.02 mmol) and $Cu(OAc)_2{\cdot}H_2O$ (3.99 mg, 0.02 mmol) were dissolved in pyridine (7 mL) and stirred for 10 min. The reaction was stopped after checking for a new green spot on the TLC. Then the pyridine was evaporated under reduced pressure and the crude product was purified by silica gel column chromatography. The desired compound was eluted in a 15% DCM–pet ether mixture, and evaporation of the solvents produced dyad **5** as a dark brown solid, in 89% yield (18 mg). Mp > 300 °C; R_f = 0.40 (silica, DCM–hexane 1 : 5); ^{1}H NMR (CD_2Cl_2, 500 MHz, δ ppm): 8.25 (s, 1H, carbazole Ar), 8.03 (d, J = 7 Hz, 1H, carbazole Ar), 7.90 (s, 2H, Ar), 7.62 (m, 3H, β-pyrrole & carbazole Ar), 7.52 (d, J = 6.5 Hz, 2H, Ar), 7.39 (m, 5H, β-pyrrole and carbazole Ar), 7.20 (s, 5H, β-pyrrole & carbazole Ar), 4.3 (t, J = 7 Hz, 2H, N–CH_2), 1.89 (m, 2H, CH_2), 1.41 (m, 2H, CH_2), 0.87 (t, J = 7.3 Hz, 3H, CH_3); ^{13}C NMR ($CDCl_3$, 500 MHz, δ ppm): 144.98, 144.19, 140.86, 140.29, 132.34, 131.29, 130.24, 129.30, 126.18, 124.95, 124.18, 122.94, 122.88, 122.44, 120.55, 119.43, 112.87, 108.99, 92.82, 87.36, 43.01, 31.11, 20.56, 13.88; HRMS (ESI-Q-TOF): $C_{55}H_{28}N_5F_{10}Cu^+$ $[M]^+$: calcd m/z 1011.1481, found. m/z 1011.1351.

Dyad 6. Dyad **4** (30 mg, 0.031 mmol) was dissolved in ethanol (30 mL) in a 100 mL round-bottomed flask. Then $Co(OAc)_2{\cdot}4H_2O$ (35.61 mg, 0.143 mmol) and PPh_3 (37.5 mg, 0.143 mmol) were added to the reaction mixture at room

temperature, and after 10 min, the reaction mixture changed colour from green to red. Then the solvent was evaporated under reduced pressure. The desired product was purified by column chromatography on neutral alumina, using 25% DCM–petroleum ether as the solvent mixture, in 56% yield (22 mg). Mp > 300 °C; R_f = 0.36 (silica, DCM–hexane 1 : 5); ^{1}H NMR ($CDCl_3$, 500 MHz, δ ppm): 8.72 (d, J = 4.5 Hz, 2H, β-pyrrole), 8.41 (s, 1H, carbazole Ar), 8.32 (d, J = 5 Hz, 2H, β-pyrrole), 8.25 (d, J = 4.5 Hz, 2H, β-pyrrole), 8.15 (d, J = 8 Hz, 1H, carbazole Ar), 8.06 (d, J = 7.5 Hz, 1H, Ar), 8.03 (d, J = 4 Hz, 2H, β-pyrrole), 7.85 (d, J = 8 Hz, 1H, Ar), 7.79 (d, J = 7.5 Hz, 1H, Ar), 7.75 (d, J = 8.5 Hz, 1H, carbazole Ar), 7.51 (t, J = 7.5 Hz, 1H, Ar), 7.44 (m, 3H, carbazole Ar & Ar), 7.28 (t, J = 7.5 Hz, 1H, carbazole Ar), 7.03 (t, J = 7.5 Hz, 3H, axial Ph), 6.68 (t, J = 7 Hz, 6H, axial Ph), 4.64 (m, 6H, axial Ph), 4.33 (t, J = 7.5 Hz, 2H, N–CH_2), 1.88 (m, 2H, CH_2), 1.44 (m, 2H, CH_2), 0.97 (t, J = 7.5 Hz, 3H, CH_3); ^{13}C NMR ($CDCl_3$, 500 MHz, δ ppm): 151.75, 146.01, 144.36, 144.27, 141.95, 140.9, 140.24, 136.07, 131.4, 128.82, 127.18, 127.09, 124.15, 126.17, 124.15, 123.47, 123.42, 122.98, 120.84, 120.59, 119.41, 113.26, 109, 105.55, 91.83, 87.72, 43.04, 37.13, 31.21, 20.59, 13.91; MALDI-MS: $C_{55}H_{28}N_5F_{10}Co^+$ $[M - PPh_3]^+$: calcd m/z 1007.1517, found. m/z 1006.802.

Dyad 7. To a clean and dry 50 mL 3-neck round-bottomed flask, 5-(4-iodophenyl)-10,15-bis-(pentafluorophenyl)porphyrin **3** (40 mg, 0.046 mmol) was added under a nitrogen atmosphere. Then 3-ethynyl-9-butylcarbazole (22.75 mg, 0.092 mmol) was added followed by dry toluene (13 mL) and TEA (3.2 mL). After this, $Pd_2(dba)_3$ (6 mg) and $AsPh_3$ (12 mg) were added and the reaction mixture was heated at RT for 16 h. The solvent was removed from the reaction mixture on a rotary evaporator. The desired product was purified by column chromatography on neutral alumina using a 30% DCM–pet ether mixture. Removal of the solvent produced dyad **7** as a red solid, in 60% yield (25 mg). Mp > 300 °C; R_f = 0.33 (silica, DCM–hexane 2 : 3); ^{1}H NMR ($CDCl_3$, 500 MHz, δ ppm): 8.96 (d, J = 4 Hz, 2H, β-pyrrole), 8.89 (s, 4H, β-pyrrole), 8.75 (d, J = 3.5 Hz, 2H, β-pyrrole), 8.43 (s, 1H, carbazole Ar), 8.2 (d, J = 7.5 Hz, 2H, Ar), 8.14 (d, J = 7.5 Hz, 1H, carbazole Ar), 8.09 (d, J = 8 Hz, 4H, Ar), 7.96 (d, J = 7.5 Hz, 2H, Ar), 7.76 (d, J = 8 Hz, 1H, carbazole Ar), 7.55 (d, J = 7.5 Hz, 4H, Ar), 7.48–7.51 (m, 1H, carbazole Ar), 7.41 (d, J = 8.5 Hz, 2H, carbazole Ar), 7.27 (t, J = 7.5 Hz, 1H, carbazole Ar), 4.29 (t, J = 7 Hz, 2H, N–CH_2), 2.7 (s, 6H, Ar–CH_3), 1.84–1.9 (m, 2H, CH_2), 1.39–1.43 (m, 2H, CH_2), 0.96 (t, J = 7.5 Hz, 3H, CH_3), −2.74 (s, 2H, inner NH); ^{13}C NMR ($CDCl_3$, 500 MHz, δ ppm): 141.46, 140.87, 140.27, 138.71, 137.66, 134.52, 129.80, 129.38, 128.96, 127.55, 126.15, 124.22, 123.67, 122.97, 122.49, 121.30, 121.11, 120.57, 119.40, 113.12, 108.97, 108.84, 92.35, 87.46, 43, 31.12, 21.51, 13.88; HRMS (ESI-Q-TOF): $C_{64}H_{44}N_5F_5^+$ $[M + H]^+$: calcd m/z 977.3516, found. m/z 977.3538.

Dyad 8. Dyad **7** (20 mg, 0.02 mmol) and $Zn(OAc)_2{\cdot}2H_2O$ (29.63 mg, 0.135 mmol) were added to a 100 mL round-bottomed flask. Then a $CHCl_3$/MeOH (2 : 1, 6 mL) mixture was added to the RB and the reaction mixture was stirred for 4 h at room temperature. After observing a new pink spot on the TLC, the reaction was stopped and the solvent was evaporated under reduced pressure. The desired product was purified by column chromatography on neutral alumina using a 20% DCM–pet ether mixture. Removal of the solvent produced dyad **8** as a purple solid, in 76% yield (16 mg). Mp > 300 °C; R_f = 0.42 (silica, DCM–hexane 1 : 3); ^{1}H NMR ($CDCl_3$, 500 MHz, δ ppm): 9.05 (d, J = 4 Hz, 2H, β-pyrrole), 8.99 (s, 4H, β-pyrrole), 8.84 (d, J = 4 Hz, 2H, β-pyrrole), 8.41 (s, 1H, carbazole Ar), 8.22 (d, J = 7.5 Hz, 2H, Ar), 8.09 (d, J = 7 Hz, 4H, Ar), 7.97 (d, J = 7.5 Hz, 2H, Ar), 7.76 (d, J = 8 Hz, 1H, carbazole Ar), 7.56 (d, J = 7.5 Hz, 4H, Ar), 7.45–7.51 (m, 2H, carbazole Ar), 7.38–7.43 (m, 3H, carbazole Ar), 4.31 (t, J = 7 Hz, 2H, N–CH_2), 2.71 (s, 6H, Ar–CH_3), 1.85–1.91 (m, 2H, CH_2), 1.41–1.44 (m, 2H, CH_2), 0.98 (t, J = 7.5 Hz, 3H, CH_3); ^{13}C NMR ($CDCl_3$, 500 MHz, δ ppm): 150.36, 150.34, 149.92, 139.90, 137.13, 134.52, 134.41, 132.20, 132.02, 131.98, 131.65, 129.70, 129.38, 127.33, 126.10, 124.19, 123.13, 122.94, 122.48, 121.35, 121.26, 120.55, 120.20, 119.35, 113.26, 108.94, 108.82, 92, 87.68, 43.01, 31.96, 29.73, 21.56,13.92; MALDI-MS: $C_{64}H_{42}N_5F_5Zn^+$ $[M]^+$: calcd m/z 1099.265, found. m/z 1039.051.

Dyad 9. Dyad **7** (20 mg, 0.02 mmol) and $Cu(OAc)_2{\cdot}H_2O$ (32.34 mg, 0.162 mmol) were dissolved in $CHCl_3$/MeOH (1 : 1, 10 mL) and the reaction mixture was refluxed for 1 h. Then the solvent was evaporated from the reaction mixture under reduced pressure. The desired product was purified by column chromatography on neutral alumina with a 25% DCM–pet ether mixture. Drying of the solvents afforded dyad **9** as a red solid, in 62% yield (13 mg). Mp > 300 °C; R_f = 0.50 (silica, DCM–hexane 1 : 4); MALDI-MS: $C_{64}H_{42}N_5F_5Cu^+$ $[M]^+$: calcd m/z 1038.265, found. m/z 1038.262.

Acknowledgements

This work was supported by the grants received from CSIR, Govt. of India and from IIT Gandhinagar. IG thanks the Chemistry Department, IIT Bombay for CV measurements. IG is grateful to Prof. P. C. Jha from Central University Gujarat (India) for providing the optimized value of inter-nuclear distance in the dyads for energy transfer calculations. SD and NB acknowledge IIT Gandhinagar for scholarship.

Notes and references

1 R. Poalesse, in *The Porphyrin Handbook*, ed. K. M. Kadish, K. M. Smith and R. Guilard, Academic Press, New York, 2000, ch. 11, vol. 2, pp. 201–232.
2 C. Erben, S. Will and K. M. Kadish, in *The Porphyrin Handbook*, ed. K. M. Kadish, K. M. Smith and R. Guilard, Academic Press, New York, 2000, ch. 12, vol. 2, pp. 233–300.
3 D. T. Gryko, *Eur. J. Org. Chem.*, 2002, 1735.
4 L. Shi, L. Flamigni and D. T. Gryko, *Chem. Soc. Rev.*, 2009, **38**, 1635–1646.
5 H.-Y. Liu, K.-M. Peng, X.-L. Wang, L.-L. You, J. Lu, L. Zhang, H. Wang, L.-N. Ji and H.-F. Jiang, *Tetrahedron Lett.*, 2010, **51**, 3439–3442.
6 A. Ryan, B. Tuffy, S. Horn, W. J. Blau and M. O. Senge, *Tetrahedron*, 2011, **67**, 8248–8254.

7 F. Qiu, Y. Zhou, J. Liu and X. Zhang, *Dyes Pigm.*, 2006, **71**, 37.
8 Y. Zhang, L. Wang, T. Wada and H. Sasabe, *Macromolecules*, 1996, **29**, 1569–1573.
9 K.-S. Kim, S. Jeong, C. Kim, J.-Y. Ham, Y. Kwon, B.-D. Choi and Y. S. Han, *Synth. Met.*, 2009, **159**, 1870–1875.
10 M. Uekawa, Y. Miyamoto, H. Ikeda, K. Kaifu, T. Ichi and T. Nakaya, *Thin Solid Films*, 1999, **352**, 185–188.
11 C. P. Tidwell, L. A. Alexander, L. D. Fondren, K. Belmore and D. E. Nikles, *Indian J. Chem.*, 2007, **46B**, 1658.
12 Y. Liu, H. Lin, J. T. Dy, K. Tamaki, J. Nakazaki, D. Nakayama, S. Uchida, T. Kubo and H. Segawa, *Chem. Commun.*, 2011, **47**, 4010–4012.
13 X.-F. Ren, A.-M. Ren, J.-K. Feng and X. Zhou, *Org. Electron.*, 2010, **11**, 979–989.
14 D. Holten, D. F. Bocian and J. S. Lindsey, *Acc. Chem. Res.*, 2001, **35**, 57–69.
15 E. Iengo, E. Zangrando and E. Alessio, *Acc. Chem. Res.*, 2006, **39**, 841–851.
16 D. T. Gryko and B. Koszarna, *Org. Biomol. Chem.*, 2003, **1**, 350–357.
17 P. D. Rao, S. Dhanalekshmi, B. J. Littler and J. S. Lindsey, *J. Org. Chem.*, 2000, **65**, 7323–7344.
18 P. Yang, W. Wu, J. Zhao, D. Huang and X. Yi, *J. Mater. Chem.*, 2012, **22**, 20273–20283.
19 H.-Y. Zhan, H.-Y. Liu, J. Lu, A. Z. Wang, L.-L. You, H. Wang, L.-N. Ji and H.-F. Jiang, *J. Porphyrins phthalocyanines*, 2010, **14**, 150–157.
20 I. H. Wasbotten, T. Wondimagegn and A. Ghosh, *J. Am. Chem. Soc.*, 2002, **124**, 8104–8116.
21 R. Paolesse, S. Nardis, F. Sagone and R. G. Khoury, *J. Org. Chem.*, 2001, **66**, 550–556.
22 R. W. Wagner, T. E. Johnson, F. Li and J. S. Lindsey, *J. Org. Chem.*, 1995, **60**, 5266–5273.
23 P. Thamyongkit, L. Yu, K. Padmaja, J. Jiao, D. F. Bocian and J. S. Lindsey, *J. Org. Chem.*, 2006, **71**, 1156–1171.
24 M. J. Zöllner, E. Becker, U. Jahn, W. Kowalsky and H.-H. Johannes, *Eur. J. Org. Chem.*, 2010, 4426–4435.
25 T. Ding, E. A. Alemán, D. A. Modarelli and C. J. Ziegler, *J. Phys. Chem. A*, 2005, **109**, 7411–7417.
26 A. M. Asiri, S. A. Khan, M. S. Al-Amoudi and K. A. Alamry, *Bull. Korean Chem. Soc.*, 2012, **33**, 1900.
27 A. Ghosh and K. Jynge, *Chem. – Eur. J.*, 1997, **3**, 823–833.
28 N. C. Maiti and M. Ravikanth, *J. Chem. Soc., Faraday Trans.*, 1996, **92**, 1095–1100.
29 S. Tobita, Y. Kaizu, H. Kobayashi and I. Tanaka, *J. Chem. Phys.*, 1984, **81**, 2962–2969.
30 B. Li, J. Li, Y. Fu and Z. Bo, *J. Am. Chem. Soc.*, 2004, **126**, 3430–3431.
31 B. Li, X. Xu, M. Sun, Y. Fu, G. Yu, Y. Liu and Z. Bo, *Macromolecules*, 2005, **39**, 456–461.
32 C. Thivierge, J. Han, R. M. Jenkins and K. Burgess, *J. Org. Chem.*, 2011, **76**, 5219–5228.
33 G.-S. Jiao, L. H. Thoresen and K. Burgess, *J. Am. Chem. Soc.*, 2003, **125**, 14668–14669.
34 J.-S. Hsiao, B. P. Krueger, R. W. Wagner, T. E. Johnson, J. K. Delaney, D. C. Mauzerall, G. R. Fleming, J. S. Lindsey, D. F. Bocian and R. J. Donohoe, *J. Am. Chem. Soc.*, 1996, **118**, 11181–11193.
35 N. Kitamura, T. Inoque and S. Tazuke, *Chem. Phys. Lett.*, 1982, **89**, 329–332.
36 J. S. Lindsey, P. A. Brown and D. A. Siesel, *Tetrahedron*, 1989, **45**, 4845–4866.
37 S. Prathapan, T. E. Johnson and J. S. Lindsey, *J. Am. Chem. Soc.*, 1993, **115**, 7519–7520.
38 H. Du, R.-C. A. Fuh, J. Li, L. A. Corkan and J. S. Lindsey, *Photochem. Photobiol.*, 1998, **68**, 141–142.
39 S. I. Yang, J. Li, H. Sun Cho, D. Kim, D. F. Bocian, D. Holten and J. S. Lindsey, *J. Mater. Chem.*, 2000, **10**, 283–296.
40 S. I. Yang, J. Seth, T. Balasubramanian, D. Kim, J. S. Lindsey, D. Holten and D. F. Bocian, *J. Am. Chem. Soc.*, 1999, **121**, 4008–4018.
41 D. Holten, D. F. Bocian and J. S. Lindsey, *Acc. Chem. Res.*, 2001, **35**, 57–69.
42 A. Osuka, N. Tanabe, S. Kawabata, I. Yamazaki and Y. Nishimura, *J. Org. Chem.*, 1995, **60**, 7177–7185.
43 S. Huang, Y. Fang, A. Lü, G. Lu, Z. Ou and K. M. Kadish, *J. Porphyrins Phthalocyanines*, 2012, **16**, 958–967.
44 P. Bhyrappa, M. Sankar and B. Varghese, *Inorg. Chem.*, 2006, **45**, 4136–4149.